Journal of Biomechanics 40 (2007) 1824–1831

JOURNAL OF BIOMECHANICS

www.elsevier.com/locate/jbiomech
www.JBiomech.com

Mechanical energetic contributions from individual muscles and elastic prosthetic feet during symmetric unilateral transtibial amputee walking: A theoretical study

Robert J. Zmitrewicz, Richard R. Neptune*, Kotaro Sasaki

Department of Mechanical Engineering, University of Texas at Austin, 1 University Station C2200, Austin, TX 78712, USA

Accepted 24 July 2006

Abstract

Energy storage and return (ESAR) foot-ankle prostheses have been developed in an effort to improve gait performance in lower-limb amputees. However, little is known about their effectiveness in providing the body segment mechanical energetics normally provided by the ankle muscles. The objective of this theoretical study was to use muscle-actuated forward dynamics simulations of unilateral transtibial amputee and non-amputee walking to identify the contributions of ESAR prostheses to trunk support, forward propulsion and leg swing initiation and how individual muscles must compensate in order to produce a normal, symmetric gait pattern. The simulation analysis revealed the ESAR prosthesis provided the necessary trunk support, but it could not provide the net trunk forward propulsion normally provided by the plantar flexors and leg swing initiation normally provided by the biarticular gastrocnemius. To compensate, the residual leg gluteus maximus and rectus femoris delivered increased energy to the trunk for forward propulsion in early stance and late stance into pre-swing, respectively, while the residual iliopsoas delivered increased energy to the leg in pre- and early swing to help initiate swing. In the intact leg, the soleus, gluteus maximus and rectus femoris delivered increased energy to the trunk for forward propulsion in the first half of stance, while the iliopsoas increased the leg energy it delivered in pre- and early swing. Thus, the energy stored and released by the ESAR prosthesis combined with these muscle compensations was able to produce a normal, symmetric gait pattern, although various neuromuscular and musculoskeletal constraints may make such a pattern non-optimal.
© 2006 Elsevier Ltd. All rights reserved.

Keywords: Forward dynamics simulations; Gait; Mechanical energetics; Compensatory strategies

1. Introduction

Unilateral transtibial amputee gait is often characterized by decreased walking speed, bilateral asymmetry and increased metabolic cost relative to non-amputees walking at the same speed (Ganguli et al., 1974; Hurley et al., 1990; Sanderson and Martin, 1997; Torburn et al., 1990). As a result, energy storage and return (ESAR) foot-ankle prostheses have been developed in an effort to improve gait performance. ESAR prostheses are designed to store elastic energy in early and mid stance and release it in late stance and pre-swing to provide some of the mechanical energy normally provided by the plantar flexors. This energy is deemed critical to help produce a normal gait pattern, as the plantar flexors have been shown to be important contributors to trunk support, forward propulsion and leg swing initiation in late stance (Neptune et al., 2001; Zajac et al., 2003). Previous studies have increased our understanding of the compensatory mechanisms used in transtibial amputee gait (e.g., Isakov et al., 2001; Underwood et al., 2004; Winter and Sienko, 1988). However, little is known regarding the specific contributions of ESAR prostheses to trunk support, forward propulsion and leg swing initiation normally provided by the plantar flexors, and to what extent individual muscles must compensate to restore normal walking mechanics.

Previous biomechanical studies analyzing the effectiveness of ESAR foot-ankle prostheses generally have not found statistically significant improvements relative to

*Corresponding author. Tel.: +1 512 471 0848; fax: +1 512 471 8727.
E-mail address: rneptune@mail.utexas.edu (R.R. Neptune).

0021-9290/$ - see front matter © 2006 Elsevier Ltd. All rights reserved.
doi:10.1016/j.jbiomech.2006.07.009

conventional non-ESAR (e.g., solid-ankle cushion-heel or "SACH") prostheses in quantities such as walking speed, stride length, cadence, muscle activity and energy expenditure (for a comprehensive review, see Hafner et al., 2002). The lack of significant gait improvements may be related to the inability of ESAR prostheses to replace the different energetic contributions of the uniarticular and biarticular plantar flexor muscles to the functional task requirements in walking.

Recent modeling and simulation analyses have shown that the uniarticular soleus and biarticular gastrocnemius have distinctly different biomechanical functions during stance (e.g., Neptune et al., 2001; Zajac et al., 2003). During mid single leg stance, the soleus and gastrocnemius act isometrically to provide trunk support by transferring power between the trunk and leg, but in opposite directions. The soleus decelerates the leg while accelerating the trunk forward and the gastrocnemius decelerates the trunk while accelerating the leg forward. During late stance and pre-swing, both the soleus and gastrocnemius undergo concentric activity, with energy from the soleus being primarily delivered to the trunk to provide forward propulsion and energy from the gastrocnemius being primarily delivered to the leg to accelerate it into swing. It is unclear to what extent an ESAR prosthesis is able to provide these different biomechanical functions, and the extent other muscles must compensate to restore normal walking mechanics.

The overall objective of this study was to use a detailed musculoskeletal model and forward dynamics simulations of amputee and non-amputee walking to identify the contributions of an ESAR prosthesis to trunk support, forward propulsion and leg swing initiation and how individual muscles must compensate in order to produce a normal, symmetric gait pattern. In addition, we investigated whether it is theoretically possible to produce a symmetric gait pattern with relatively normal non-amputee excitation patterns.

2. Methods

2.1. Musculoskeletal model

A previously described 2D musculoskeletal model (Fig. 1) and dynamic optimization framework (e.g., Neptune et al., 2001) were used to generate simulations of unilateral transtibial amputee and non-amputee walking at 1.5 m/s. The musculoskeletal model and simulations were generated using SIMM/Dynamics Pipeline (MusculoGraphics, Inc., Santa Rosa, CA) and consisted of rigid segments representing the trunk and legs, with each leg consisting of a thigh, shank, patella and foot. The trunk segment included the mass and inertial characteristics of the pelvis, torso, head and arms. The model was dimensioned to represent a male subject with a height of 180 cm and mass of 75 kg. Musculoskeletal geometry was based on that of Delp et al. (1990) and segment masses and inertial

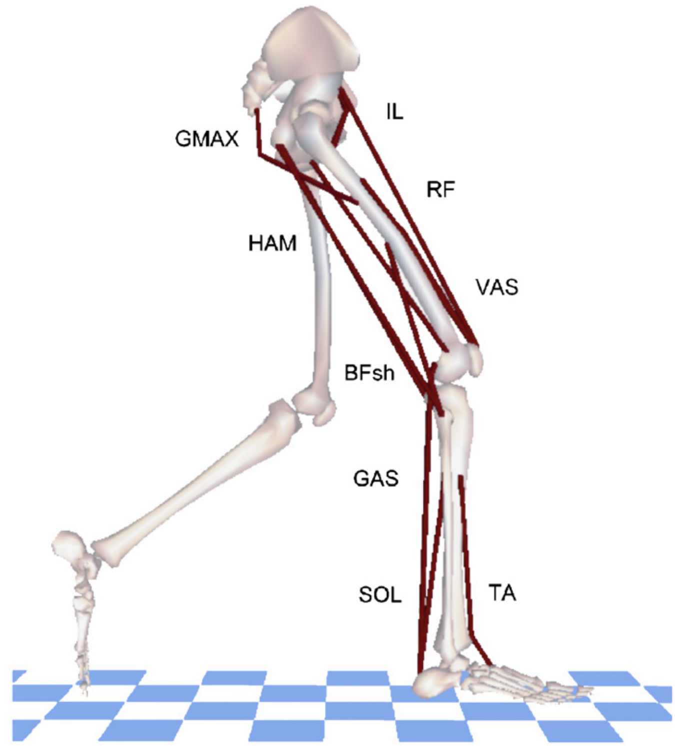

Fig. 1. Musculoskeletal model used in amputee and non-amputee simulations. The model was actuated with 15 individual muscle actuators per leg that were combined into 9 muscle groups based on anatomical classification, with muscles within each group receiving the same excitation signal. The muscle groups in the model were defined as SOL (soleus), GAS (medial, lateral gastrocnemius), HAM (biceps femoris long head, semimembranosus), BFsh (biceps femoris short head), IL (psoas, iliacus), TA (tibialis anterior), RF (rectus femoris), VAS (3-component vasti) and GMAX (gluteus maximus, adductor magnus).

properties were determined using regression equations (Chandler et al., 1975; Clauser et al., 1969). In the amputee model, the inertial characteristics of the residual leg were determined using data in Mattes et al. (2000).

The trunk was allowed to translate and rotate in the sagittal plane. The hip and ankle joints were modeled as frictionless revolutes while the knee joint had a moving center-of-rotation for flexion and extension and the patella had a prescribed trajectory relative to the femur, which were both defined as functions of the knee flexion angle (Delp et al., 1990). The model had a total of nine degrees-of-freedom. Passive torques representing the forces applied by ligaments, passive tissue and joint structures were applied at the hip, knee and ankle joints based on Davy and Audu (1987). Contact between the foot and ground was modeled by 30 independent visco-elastic elements with coulomb friction attached to each foot segment (Neptune et al., 2000). The equations-of-motion were generated using SD/FAST (PTC, Needham, MA).

The muscle contractile dynamics were governed by Hill-type muscle properties including the force–length–velocity–activation relationships (Schutte et al., 1993). For the amputee simulation, the model was modified by removing the ankle plantar flexors and tibialis anterior from the residual leg and replacing them with a visco-elastic torsional spring at the ankle joint with a stiffness of a nominal ESAR prosthesis (Klute et al., 2001, modified from Lehman et al., 1993) as

$$T = -600\theta_A - 15\omega_A, \tag{1}$$

where θ_A is the ankle angle (rad) and ω_A the ankle angular velocity (rad/s), with the corresponding terms representing the stiffness and damping, respectively. Muscle excitations were modeled using block patterns with four excitation nodes per muscle with the exception of RF, which was given a two burst pattern with one magnitude level each during late swing-early stance and pre- and early swing. The muscle activation dynamics were modeled by a first-order differential equation (Raasch et al., 1997) with activation and deactivation time constants of 50 and 65 ms, respectively.

2.2. Dynamic optimization

Amputee and non-amputee walking simulations of a complete gait cycle were generated by solving the optimal tracking problem (e.g., Neptune and Hull, 1998) using a simulated annealing algorithm (Goffe et al., 1994) to determine the muscle controls (i.e., individual muscle excitation onset, duration and magnitude) such that the simulations emulated non-amputee experimentally measured kinematic and ground reaction force data. The muscle onset and offset timing between legs was assumed symmetric (50% of the gait cycle out-of-phase) and constrained to match non-amputee EMG timing within $\pm 10\%$ of the gait cycle (Perry, 1992). In the amputee simulation, the excitation magnitudes were allowed to vary between legs. The objective function was formulated to minimize the squared error normalized by the inter-trial variability for each quantity tracked. The objective function was defined as

$$J = \sum_{j=1}^{m} \sum_{i=1}^{n} \frac{(Y_{ij} - \hat{Y}_{ij})^2}{\mathrm{SD}_{ij}^2}, \tag{2}$$

where Y_{ij} is the experimental measurement of variable j at time step i, $\hat{Y}_{ij}$ the simulation data corresponding to Y_{ij}, and SD_{ij}^2 the average inter-subject variability of variable j at time step i. Specific quantities evaluated in the objective function included hip, knee and ankle joint angles, pelvis rotation, trunk translation in both the x- and y-directions, and horizontal and vertical ground reaction forces. The amputee (non-amputee) simulation began with residual (ipsilateral) leg heel-strike and concluded with the second residual (ipsilateral) leg heel-strike.

2.3. Experimental data collection

The experimental tracking data were collected from 10 non-amputee subjects (5 male, 5 female; age 29.6 ± 6.1 years; height 169.7 ± 10.9 cm; mass 65.6 ± 10.7 kg) walking at 1.5 m/s on a split-belt instrumented treadmill (Tecmachine, Cedex, France). A motion capture system was used to collect three-dimensional ground reaction force and body segment motion data (Motion Analysis, Corp., Santa Rosa, CA) at 480 and 120 Hz, respectively, for 15 s. Body segment motion data were measured using a modified Helen Hayes marker set (described in McLean et al., 2005) and corresponding joint angles were calculated. The ground reaction force and kinematic data were filtered with a fourth-order zero-lag Butterworth filter with cut-off frequencies of 20 and 6 Hz, respectively. All data were time-normalized to a full gait cycle, averaged for each subject, and then averaged across subjects to provide a group average. Prior to data collection, all subjects provided informed consent according to the rules and regulations of the Cleveland Clinic Foundation and The University of Texas at Austin.

2.4. Assessing muscle and prosthesis function

In order to quantify how the ESAR prosthesis and individual muscles work in synergy to satisfy the mechanical energetic demands of walking, a segment power analysis (Fregly and Zajac, 1996) was performed to quantify their contributions to the accelerations and mechanical power of the individual body segments. Positive power delivered by a muscle or the ESAR prosthesis to a segment indicates that it acted to accelerate the segment in the direction of its motion, while negative power indicates that it acted to decelerate the segment motion. In addition, individual musculotendon work over the gait cycle was quantified by integrating the musculotendon power during the swing phase and first and second half of stance. Similarly, the amount of energy stored and returned by the prosthesis was quantified by integrating the negative and positive prosthesis power, respectively.

3. Results

Both the non-amputee and amputee simulations emulated well the group-averaged kinematics and ground reaction forces throughout most of the gait cycle (Fig. 2). Thus, the energy stored and returned by the ESAR prosthesis and various muscle compensations were able to produce a normal, symmetric gait pattern with non-amputee excitation patterns. The prosthesis stored mechanical energy throughout most of stance (primarily as the trunk moved over the foot and bodyweight acted to dorsiflex the ankle joint; Fig. 3: 10–80% stance phase, solid line < 0) before releasing it in late stance and pre-swing (Fig. 3: 80–100% stance phase, solid line > 0). The mechanical energy released by the prosthesis (12.0 J) was less than half that delivered by SOL and GAS (28.3 J) during the same region in the non-amputee simulation (Table 1) (Fig. 3: 75–100% stance phase, compare solid line to sum of dash–dot and dotted lines).

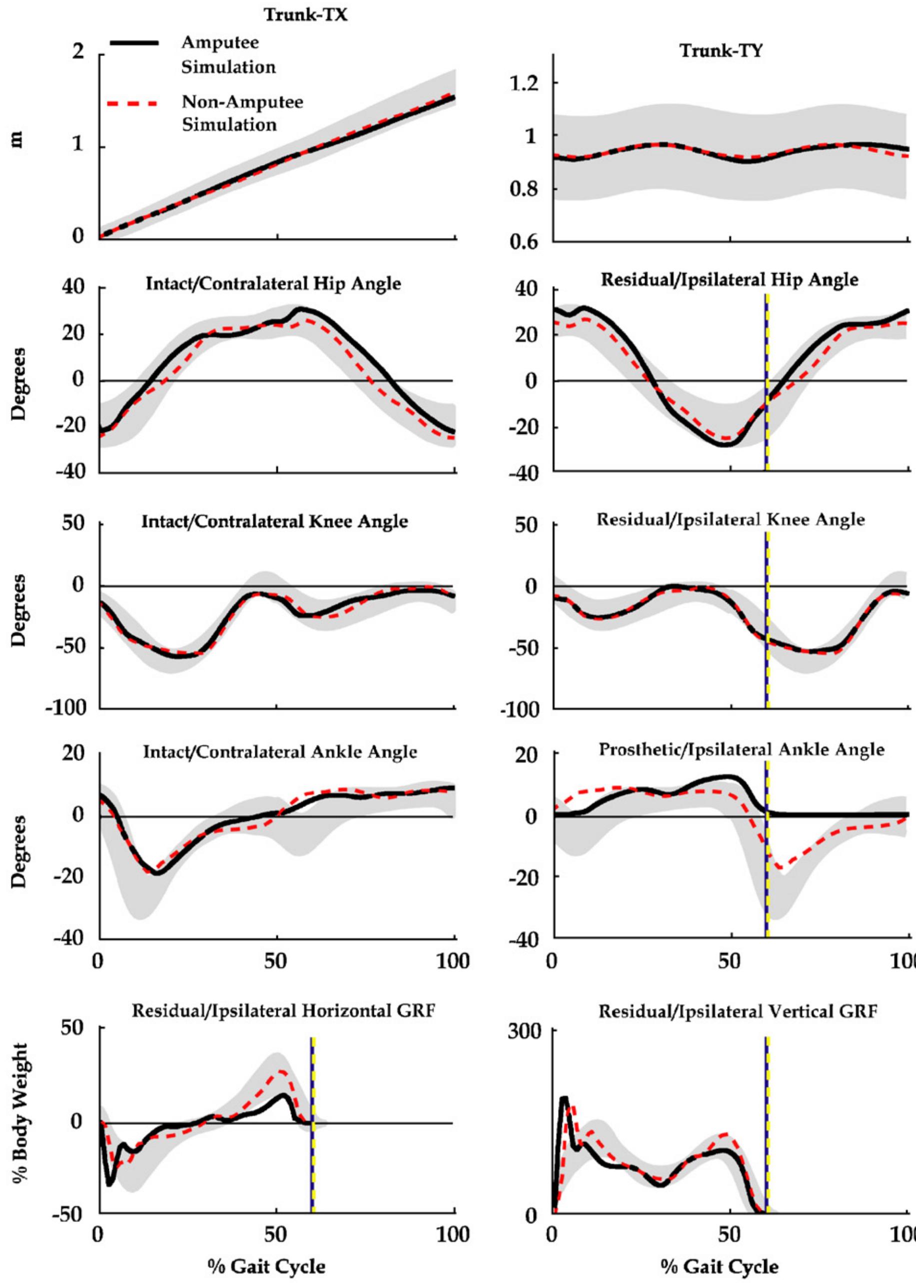

Fig. 2. Comparison of the amputee (solid line) and non-amputee (dashed line) simulations with the group averaged experimental data (shaded region). The experimental data represent the average of the 10 non-amputee subjects $\pm$2SD. The solid vertical line denotes the end of residual leg stance phase while the dashed line denotes the end of ipsilateral leg stance. All joint angles are plotted with respect to the residual leg gait cycle.

From a biomechanical perspective, the prosthesis functioned similarly to the uniarticular SOL throughout most of stance. From early to mid stance, as SOL was near isometric and the prosthesis began to store elastic energy (Fig. 3: 10–40% stance phase, dash–dot line near 0, solid line <0), both provided trunk support (i.e., accelerated the trunk upward) (Fig. 4C: 10–40% stance phase, dashed and dash–dot lines >0). From mid to late stance, both the prosthesis and SOL transferred energy from the leg to the trunk (Fig. 4A: 50–85% stance phase, dotted and dash–dot lines <0, solid lines >0), which acted to decelerate the downward motion of the trunk (Fig. 4C: 50–85% stance phase, dashed and dash–dot lines <0) while simultaneously providing forward propulsion (Fig. 4C: 50–85% stance phase, SOL and prosthesis solid lines >0). In pre-swing, both SOL and the prosthesis provided energy to both the leg and trunk (Fig. 4A: 85–100% stance phase, all lines >0), which provided both trunk support and forward propulsion (Fig. 4C: 85–100% stance phase).

Although the ESAR prosthesis was able to provide the primary functions of SOL, it could not provide all the functions of GAS. From late stance into pre-swing, GAS delivered power to the leg to accelerate it into swing (Fig. 4B: 70–95% stance phase, dash-dot line > 0). However, the prosthesis acted to decelerate the leg much from mid- to late stance similar to SOL (Fig. 4D: 40–85% stance phase, prosthesis and SOL solid lines < 0) and could only deliver a small amount of energy to the leg during pre-swing (Fig. 4B: 85–100% stance phase, dotted line > 0). To compensate, the residual leg IL increased its energy delivered to the leg in pre- and early swing relative to the non-amputee IL to help accelerate the leg into swing (50.0 vs. 38.1 J, respectively; Table 2, sum of second half of stance and swing values).

The trunk support provided by the prosthesis was sufficient to replace that of the combined ankle plantar flexors (Fig. 4C: 50–85% stance phase, compare dash–dot line with the sum of the dashed and dotted lines). The trunk forward propulsion provided by the prosthesis in the second half of stance was also similar to that provided by the combined plantar flexors (Fig. 4C: 50–90% stance phase, compare solid lines); however, the prosthesis decelerated the forward motion of the trunk to a greater extent in the first half of stance (Fig. 4C: 0–50% stance phase, compare solid lines). Thus, the net trunk propulsion provided by the prosthesis was less than that provided by the plantar flexors. As a result, compensations from various muscle groups were needed to provide additional forward propulsion. One compensation occurred in the residual leg RF, which increased its excitation and acted to transfer more energy from the leg to the trunk (Table 2) (Fig. 5A: 30–60% gait cycle, dotted line < 0, solid line > 0) to provide forward propulsion in late stance and pre-swing (Fig. 5B: 30–60% gait cycle, solid line > 0). A second compensation occurred during early residual leg stance. The residual leg GMAX increased its excitation and delivered 17.5 J to the trunk for forward propulsion, compared to 11.3 J delivered in the non-amputee simulation (Table 2).

Additional compensations occurred in the intact leg. During the first half of intact leg stance, the intact RF, GMAX and SOL all delivered more energy from the leg to the trunk to provide forward propulsion compared to the non-amputee simulation (Table 2). In addition, during pre- and early swing, the intact leg IL delivered more energy to the leg (53.3 vs. 38.1 J; Table 2, sum of second half of stance and swing values).

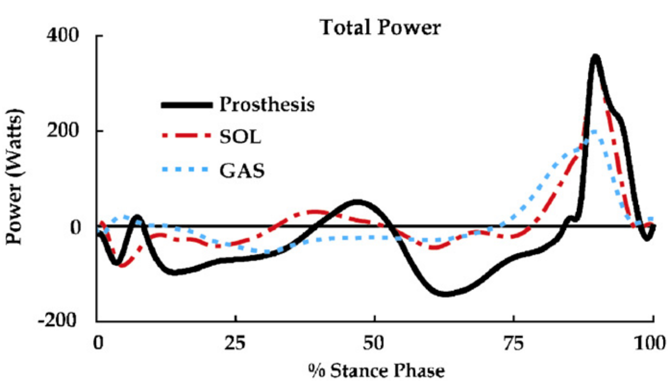

Fig. 3. Total mechanical power (i.e., the sum of the horizontal, vertical and rotational power) from the non-amputee SOL, non-amputee GAS and ESAR prosthesis.

4. Discussion

Previous studies have shown ESAR prostheses are effective devices for storing and returning mechanical energy relative to conventional prostheses (e.g., Ehara et al., 1993; Prince et al., 1998). However, little is known about what functional tasks are provided by ESAR prostheses and to what extent individual muscles must compensate to produce a normal, symmetric gait pattern. Therefore, the overall objective of this study was to use simulations of amputee and non-amputee walking to identify the contributions of an ESAR prosthesis to trunk support, forward propulsion and swing initiation and the corresponding muscle compensations that need to occur. A secondary goal was to assess whether it is theoretically possible to produce a symmetric gait pattern with relatively normal non-amputee excitation patterns. The results

Table 1
Total mechanical energy stored (negative) and returned (positive) by the ESAR prosthesis compared to the positive and negative work by the non-amputee and intact leg SOL and GAS

	Total energy (J)					
	First half stance		Second half stance		Swing	
	+	−	+	−	+	−
Prosthesis	2.3	−13.7	12.0	−14.1	0.0	0.0
Non-amputee SOL	2.0	−6.1	14.4	−3.3	0.0	−2.6
Non-amputee GAS	0.5	−7.2	13.9	−2.2	0.0	−5.7
Intact SOL	0.0	−7.7	18.0	−2.5	0.0	−4.4
Intact GAS	0.0	−8.9	16.1	−0.6	0.0	−5.7

The energy returned by the prosthesis during late stance was less than half that produced by the non-amputee SOL and GAS. The mechanical efficiency of the prosthesis (energy returned/energy stored) was 51%.

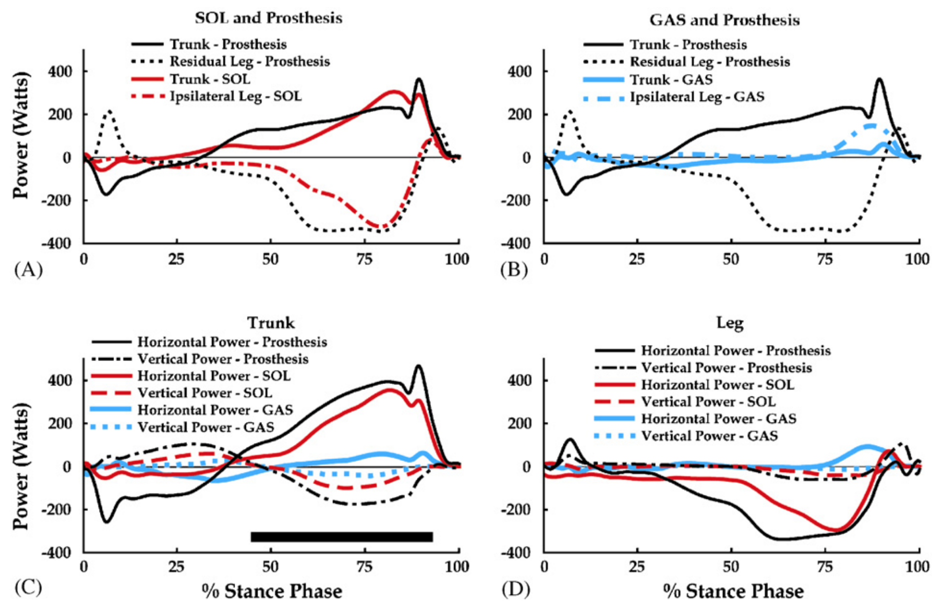

Fig. 4. (A) Total mechanical power output from the ESAR *prosthesis* and *SOL* in the non-amputee simulation. Total power is the sum of horizontal, vertical and rotational power. Power to the ''leg'' is the sum of the femur, tibia, patella and foot segments. (B) Mechanical power output from the ESAR *prosthesis* and *GAS* in the non-amputee simulation. (C) Horizontal and vertical power output to the trunk by the ESAR *prosthesis* and *SOL* and *GAS* from the non-amputee simulation. Positive (negative) power to the leg/trunk indicates that the muscle or prosthesis accelerated (decelerated) the leg/trunk in the direction of its motion. The horizontal bar indicates when the trunk is moving downward. (D) Horizontal and vertical power output to the residual leg by the ESAR *prosthesis* and to the ipsilateral leg from the *SOL* and *GAS* in the non-amputee simulation. Horizontal power delivered to the leg in late stance helps provide swing initiation.

Table 2
Mechanical energy provided to the trunk and residual, intact and non-amputee legs by the corresponding SOL, RF, IL and GMAX

	Energy to leg/trunk (J)											
	First half stance				Second half stance				Swing			
	Leg		Trunk		Leg		Trunk		Leg		Trunk	
	+	−	+	−	+	−	+	−	+	−	+	−
Intact SOL	0.0	−21.4	12.6	−0.8	3.3	−36.4	42.6	0.0	0.1	−4.7	1.2	−1.2
Non-amputee SOL	0.0	−8.4	6.7	−2.7	2.0	−40.3	43.2	0.0	0.2	−4.1	1.4	−0.4
Residual RF	0.0	−2.9	1.7	0.0	0.0	−36.2	17.1	0.0	0.7	−0.4	0.4	0.0
Intact RF	0.0	−9.4	6.4	0.0	0.0	−14.2	7.9	0.0	1.0	−0.7	1.6	0.0
Non-amputee RF	0.0	−4.2	2.0	0.0	0.0	−15.2	8.0	0.0	0.7	−1.0	2.1	0.0
Residual IL	2.0	0.0	0.5	−5.2	27.1	0.0	0.5	−7.5	22.9	0.0	0.0	−11.2
Intact IL	2.0	0.0	0.1	−3.9	21.2	0.0	0.2	−7.4	32.1	0.0	0.0	−14.2
Non-amputee IL	1.2	0.0	0.6	−3.2	12.2	0.0	0.0	−5.9	25.9	0.0	0.0	−10.5
Residual GMAX	0.8	−7.1	17.5	−7.2	0.5	−2.0	0.3	−0.4	0.0	−5.4	4.4	0.0
Intact GMAX	0.0	−8.3	16.6	−0.1	0.2	−1.3	0.3	−0.2	0.0	−4.0	1.6	0.0
Non-amputee GMAX	0.9	−4.4	11.3	−4.3	0.2	−0.9	0.2	−0.1	0.0	−4.1	1.6	0.0

showed that a symmetric gait pattern was possible despite the loss of the important plantar flexor muscles; however, muscle compensations in both the residual and intact leg were necessary.

The prosthesis was modeled using the stiffness of a nominal ESAR prosthesis that had a mechanical efficiency of 51% (Table 1; ratio of energy returned versus stored), which was comparable to values reported in previous studies ranging from 20–67% (e.g., Barr et al., 1992; Ehara et al., 1993; Prince et al., 1998). The energy returned by the prosthesis in the second half of stance (12.0 J) was within the range of published values for a similar Flex-Foot ESAR prostheses (e.g., 9.3 J in Ehara et al., 1993; 16.2 J in Gitter et al., 1991).

The simulation analysis showed that the ESAR prosthesis stored elastic energy through most of stance and

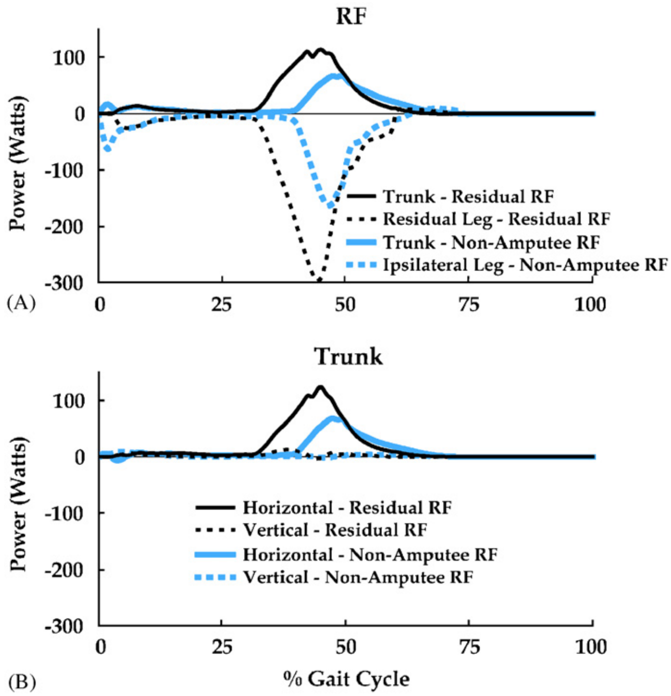

Fig. 5. (A) Mechanical power delivered by the non-amputee and residual RF. (B) Horizontal and vertical power output to the trunk by the non-amputee and residual RF.

returned some of that energy in late stance and pre-swing (Fig. 3: solid line). Biomechanically, the ESAR prosthesis provided the trunk support throughout stance and forward propulsion in the second half of stance normally provided by the plantar flexors (Fig. 4C). However, the prosthesis decelerated the trunk in the horizontal direction to a greater extent in the first half of stance compared to SOL and GAS (Fig. 4C), and therefore could not replace the net propulsion provided by the plantar flexors. Thus, additional energy for forward propulsion was necessary to maintain the required walking speed. The primary compensatory mechanism in late stance and pre-swing was an increase in residual leg RF excitation, which transferred additional energy from the leg to the trunk to provide forward propulsion (Table 2; Fig. 5B). Much of the increased leg energy transferred by RF was provided by the residual IL, which acts to redistribute energy from the trunk to the leg, as well as generate energy directly to the leg (Neptune et al., 2004; Zajac et al., 2003). Increased residual leg hip flexor power output was similarly observed in Sadeghi et al. (2001). A second compensation occurred during early residual leg stance as the residual leg GMAX increased its excitation to deliver additional energy to the trunk (Table 2) for forward propulsion (Neptune et al., 2004; Zajac et al., 2003). This was consistent with previous studies showing increased residual leg hip extensor power (Bateni and Olney, 2002; Gitter et al., 1991; Sadeghi et al., 2001) and gluteus maximus EMG activity (Winter and Sienko, 1988) during amputee walking.

Additional muscle compensations occurred in the intact leg. During the first half of intact leg stance, the intact SOL, RF and GMAX all delivered more energy from the leg to the trunk (Table 2) to provide forward propulsion (Neptune et al., 2001; Neptune et al., 2004). The increased SOL, RF and GMAX output was consistent with previous studies showing increased ankle plantar flexor (Bateni and Olney, 2002; Lemaire et al., 1993), knee extensor (Bateni and Olney, 2002; Nolan and Lees, 2000), and hip extensor (Bateni and Olney, 2002; Sadeghi et al., 2001) moment and/or power output in the intact leg during this region. In addition, the intact leg IL generated more energy to the intact leg in pre- and early-swing (Table 2), which was consistent with previous studies showing increased hip flexor moment and/or power output in the intact leg during this region (Bateni and Olney, 2002; Lemaire et al., 1993).

The prosthesis did not provide the swing initiation normally provided by GAS in pre-swing, which was consistent with previous studies showing amputees exhibit a decreased cadence and stride length compared to non-amputees (Barth et al., 1992; Skinner and Effeney, 1985) and no significant change in amputee cadence (Powers et al., 1994; Snyder et al., 1995) or residual leg stride length (Barr et al., 1992; Lehmann et al., 1993; Schmalz et al., 2002) when wearing ESAR prostheses versus conventional non-energy storing prostheses. Therefore, in order to produce a symmetric gait pattern, greater residual leg IL activity was needed to accelerate the leg into swing to provide the necessary leg swing kinematics, as well as provide the additional energy transferred from the leg to the trunk by the residual RF (Fig. 5).

The simulation results showed that the energy stored and released in an ESAR prosthesis combined with muscle compensations in both the intact and residual legs can produce a normal, symmetric gait pattern using similar excitation patterns as non-amputees. However, decreases in muscle strength, altered neural control and sensory feedback and other neuromuscular and musculoskeletal disorders may place constraints on the nervous system that make a symmetric gait pattern non-optimal. In addition, the present study identified one compensatory strategy, but others may exist. Future work will be directed at verifying whether amputees who walk with symmetric gait patterns use similar strategies as those found in the present study and identifying the range of strategies that may exist.

Acknowledgment

This work was supported by National Science Foundation Grant BES-0346514.

References

Barr, A.E., Siegel, K.L., Danoff, J.V., McGarvey III, C.L., Tomasko, A., Sable, I., Stanhope, S.J., 1992. Biomechanical comparison of the energy-storing capabilities of SACH and Carbon Copy II prosthetic feet during the stance phase of gait in a person with below-knee amputation. Physical Therapy 72, 344–354.

Barth, D.G., Schumacher, L., Thomas, S., 1992. Gait analysis and energy cost of below-knee amputees wearing six different prosthetic feet. Journal of Prosthetics and Orthotics 4, 63–75.

Bateni, H., Olney, S.J., 2002. Kinematic and kinetic variations of below-knee amputee gait. Journal of Prosthetics and Orthotics 14, 1–7.

Chandler, R.F., Clauser, C.E., McConville, J.T., Reynolds, H.M., Young, J.W., 1975. Investigation of Intertial Properties of the Human Body. Wright Patterson Air Force Base, Ohio (AMRL-TR-75-137).

Clauser, C.E., McConville, J.T., Young, J.W., 1969. Weight, Volume, and Center of Mass of Segments of the Human Body. Wright Patterson Air Force Base, Ohio (AMRL-TR-69-70).

Davy, D.T., Audu, M.L., 1987. A dynamic optimization technique for predicting muscle forces in the swing phase of gait. Journal of Biomechanics 20, 187–201.

Delp, S.L., Loan, J.P., Hoy, M.G., Zajac, F.E., Topp, E.L., Rosen, J.M., 1990. An interactive graphics-based model of the lower extremity to study orthopaedic surgical procedures. IEEE Transactions on Biomedical Engineering 37, 757–767.

Ehara, Y., Beppu, M., Nomura, S., Kunimi, Y., Takahashi, S., 1993. Energy storing property of so-called energy-storing prosthetic feet. Archives of Physical Medicine and Rehabilitation 74, 68–72.

Fregly, B.J., Zajac, F.E., 1996. A state-space analysis of mechanical energy generation, absorption, and transfer during pedaling. Journal of Biomechanics 29, 81–90.

Ganguli, S., Datta, S.R., Chatterjee, B.B., Roy, B.N., 1974. Metabolic cost of walking at different speeds with patellar tendon-bearing prosthesis. Journal of Applied Physiology 36, 440–443.

Gitter, A., Czerniecki, J.M., DeGroot, D.M., 1991. Biomechanical analysis of the influence of prosthetic feet on below-knee amputee walking. American Journal of Physical Medicine and Rehabilitation 70, 142–148.

Goffe, W.L., Ferrier, G.D., Rogers, J., 1994. Global optimization of statistical functions with simulated annealing. Journal of Econometrics 60, 65–99.

Hafner, B.J., Sanders, J.E., Czerniecki, J., Fergason, J., 2002. Energy storage and return prostheses:does patient perception correlate with biomechanical analysis? Clinical Biomechanics 17, 325–344.

Hurley, G.R., McKenney, R., Robinson, M., Zadravec, M., Pierrynowski, M.R., 1990. The role of the contralateral limb in below-knee amputee gait. Prosthetics and Orthotics International 14, 33–42.

Isakov, E., Burger, H., Krajnik, J., Gregoric, M., Marincek, C., 2001. Knee muscle activity during ambulation of trans-tibial amputees. Journal of Rehabilitation Medicine 33, 196–199.

Klute, G.K., Kallfelz, C.F., Czerniecki, J.M., 2001. Mechanical properties of prosthetic limbs: adapting to the patient. Journal of Rehabilitation Research and Development 38, 299–307.

Lehmann, J.F., Price, R., Boswell-Bessette, S., Dralle, A., Questad, K., deLateur, B.J., 1993. Comprehensive analysis of energy storing prosthetic feet: Flex Foot and Seattle Foot versus standard SACH foot. Archives of Physical Medicine and Rehabilitation 74, 1225–1231.

Lemaire, E.D., Fisher, F.R., Robertson, D.G., 1993. Gait patterns of elderly men with trans-tibial amputations. Prosthetics and Orthotics International 17, 27–37.

Mattes, S.J., Martin, P.E., Royer, T.D., 2000. Walking symmetry and energy cost in persons with unilateral transtibial amputations: matching prosthetic and intact limb inertial properties. Archives of Physical Medicine and Rehabilitation 81, 561–568.

McLean, S.G., Huang, X., van den Bogert, A.J., 2005. Association between lower extremity posture at contact and peak knee valgus moment during sidestepping: implications for ACL injury. Clinical Biomechanics 20, 863–870.

Neptune, R.R., Hull, M.L., 1998. Evaluation of performance criteria for simulation of submaximal steady-state cycling using a forward dynamic model. Journal of Biomechanical Engineering 120, 334–341.

Neptune, R.R., Wright, I.C., Van Den Bogert, A.J., 2000. A method for numerical simulation of single limb ground contact events: application to heel-toe running. Computer Methods in Biomechanics and Biomedical Engineering 3, 321–334.

Neptune, R.R., Kautz, S.A., Zajac, F.E., 2001. Contributions of the individual ankle plantar flexors to support, forward progression and swing initiation during walking. Journal of Biomechanics 34, 1387–1398.

Neptune, R.R., Zajac, F.E., Kautz, S.A., 2004. Muscle force redistributes segmental power for body progression during walking. Gait and Posture 19, 194–205.

Nolan, L., Lees, A., 2000. The functional demands on the intact limb during walking for active trans-femoral and trans-tibial amputees. Prosthetics and Orthotics International 24, 117–125.

Perry, J., 1992. Gait Analysis: Normal and Pathological Function. Slack, Inc., Thorofare, NJ.

Powers, C.M., Torburn, L., Perry, J., Ayyappa, E., 1994. Influence of prosthetic foot design on sound limb loading in adults with unilateral below-knee amputations. Archives of Physical Medicine and Rehabilitation 75, 825–829.

Prince, F., Winter, D.A., Sjonnensen, G., Powell, C., Wheeldon, R.K., 1998. Mechanical efficiency during gait of adults with transtibial amputation: a pilot study comparing the SACH, Seattle, and Golden-Ankle prosthetic feet. Journal of Rehabilation Research and Development 35, 177–185.

Raasch, C.C., Zajac, F.E., Ma, B., Levine, W.S., 1997. Muscle coordination of maximum-speed pedaling. Journal of Biomechanics 30, 595–602.

Sadeghi, H., Allard, P., Duhaime, P.M., 2001. Muscle power compensatory mechanisms in below-knee amputee gait. American Journal of Physical Medicine and Rehabilitation 80, 25–32.

Sanderson, D.J., Martin, P.E., 1997. Lower extremity kinematic and kinetic adaptations in unilateral below-knee amputees during walking. Gait and Posture 6, 126–136.

Schmalz, T., Blumentritt, S., Jarasch, R., 2002. Energy expenditure and biomechanical characteristics of lower limb amputee gait: the influence of prosthetic alignment and different prosthetic components. Gait and Posture 16, 255–263.

Schutte, L.M., Rodgers, M.M., Zajac, F.E., Glaser, R.M., 1993. Improving the efficacy of electrical stimulation-induced cycle ergonometry: an analysis based on dynamic musculoskeletal model. IEEE Transactions on Rehabilitation Engineering 1, 109–125.

Skinner, H.B., Effeney, D.J., 1985. Gait analysis in amputees. American Journal of Physical Medicine 64, 82–91.

Snyder, R.D., Powers, C.M., Fontaine, C., Perry, J., 1995. The effect of five prosthetic feet on the gait and loading of the sound limb in dysvascular below-knee amputees. Journal of Rehabilitation Research and Development 32, 309–315.

Torburn, L., Perry, J., Ayyappa, E., Shanfield, S.L., 1990. Below-knee amputee gait with dynamic elastic response prosthetic feet: a pilot study. Journal of Rehabilitation Research and Development 27, 369–384.

Underwood, H.A., Tokuno, C.D., Eng, J.J., 2004. A comparison of two prosthetic feet on the multi-joint and multi-plane kinetic gait compensations in individuals with a unilateral trans-tibial amputation. Clinical Biomechanics 19, 609–616.

Winter, D.A., Sienko, S.E., 1988. Biomechanics of below-knee amputee gait. Journal of Biomechanics 21, 361–367.

Zajac, F.E., Neptune, R.R., Kautz, S.A., 2003. Biomechanics and muscle coordination of human walking. Part II: lessons from dynamical simulations and clinical implications. Gait and Posture 17, 1–17.